



RESEARCH LETTER

10.1002/2016GL068390

Key Points:

- The GWP of N₂O decreases with a decline in the N₂O lifetime under climate change conditions
- With decreasing lifetime, the total radiative forcing of N₂O is reduced due to a decline in its burden
- Due to a linear dependence on temperature rise, our findings can be extended to other scenarios

Supporting Information:

- Supporting Information S1

Correspondence to:

D. Kracher,
daniela.kracher@mpimet.mpg.de

Citation:

Kracher, D., C. H. Reick, E. Manzini, M. G. Schultz, and O. Stein (2016), Climate change reduces warming potential of nitrous oxide by an enhanced Brewer-Dobson circulation, *Geophys. Res. Lett.*, 43, 5851–5859, doi:10.1002/2016GL068390.

Received 25 FEB 2016

Accepted 12 MAY 2016

Accepted article online 14 MAY 2016

Published online 4 JUN 2016

Climate change reduces warming potential of nitrous oxide by an enhanced Brewer-Dobson circulation

Daniela Kracher¹, Christian H. Reick¹, Elisa Manzini¹, Martin G. Schultz², and Olaf Stein²

¹Max Planck Institute for Meteorology, Hamburg, Germany, ²Forschungszentrum Jülich GmbH, Jülich, Germany

Abstract The Brewer-Dobson circulation (BDC), which is an important driver of the stratosphere-troposphere exchange, is expected to accelerate with climate change. One particular consequence of this acceleration is the enhanced transport of nitrous oxide (N₂O) from its sources at the Earth's surface toward its main sink region in the stratosphere, thus inducing a reduction in its lifetime. N₂O is a potent greenhouse gas and the most relevant currently emitted ozone-depleting substance. Here we examine the implications of a reduced N₂O lifetime in the context of climate change. We find a decrease in its global warming potential (GWP) and, due to a decline in the atmospheric N₂O burden, also a reduction in its total radiative forcing. From the idealized transient global warming simulation we can identify linear regressions for N₂O sink, lifetime, and GWP with temperature rise. Our findings are thus not restricted to a particular scenario.

1. Introduction

The Brewer-Dobson circulation (BDC) is characterized by upwelling of tropospheric air into the stratosphere in the tropics and downwelling of stratospheric air into the troposphere in the extratropics. It is stronger in winter and more pronounced in the northern than the southern hemisphere [Butchart, 2014].

Due to an increased transport of momentum to higher altitudes by planetary and gravity wave dissipation, the BDC is expected to accelerate under climate change according to simulation studies [Butchart *et al.*, 2006; Hardiman *et al.*, 2014]. This accelerated mass transport will affect long-lived gases having stratospheric sinks such as N₂O and chlorofluorocarbons (CFCs), which are ozone-depleting substances (ODS). Previous studies [Butchart and Scaife, 2001; Douglass *et al.*, 2008; Fleming *et al.*, 2011; Chipperfield *et al.*, 2014; Neu *et al.*, 2014] examined the effect of an enhanced BDC on ODS and ozone concentrations. However, N₂O not only plays an important role in ozone depletion [Ravishankara *et al.*, 2009], it is also the third most important anthropogenic greenhouse gas. N₂O is mainly produced by microbial processes in the soil and the ocean. Climate-N₂O interactions have so far been considered regarding changes in N₂O emissions, while implications via atmospheric dynamics have not been taken into account. The main sink of N₂O is in the stratosphere, where it is destroyed by photolysis (90%) and reaction with excited oxygen (10%). With accelerated BDC, transport of N₂O from the source regions into the stratosphere will increase, thereby enhancing the N₂O sink and thus reducing its residence time in the atmosphere. This constitutes an important factor in light of climate change, which has not been considered so far.

The lifetime of N₂O is not only affected by an enhanced circulation but also by potential changes in photolytic and chemical sink rates, which in turn depend on the stratospheric ozone concentration. Ozone chemistry is complex and involves several components. Considering all factors interfering with ozone concentrations demands specific assumptions regarding, e.g., the evolution of CO₂ concentration in the stratosphere, release of CFCs from banks, emissions, and chemical reactions of other atmospheric compounds that are directly or indirectly involved in ozone chemistry. Here we focus on the effect of an enhanced BDC, and we can thus provide results that are not restricted to specific assumptions. We specifically quantify the effect of a changing N₂O lifetime for the efficacy of N₂O as a greenhouse gas: First, we quantify how the decrease in atmospheric burden induced by an enhanced sink affects the total radiative forcing of N₂O. Second, we calculate how its global warming potential (GWP) is affected by a reduced lifetime.

2. Methods

To quantify the effect of an enhanced BDC on the atmospheric fate of N_2O , we apply ECHAM6 [Stevens *et al.*, 2013], the atmosphere model of the MPI-ESM (Max Planck Institute Earth System Model) in an idealized setup. We conduct two 100 yearlong simulations, one control simulation “CTRL” at preindustrial state and one simulation “1PCT” with 1% yearly increase in atmospheric CO_2 . Both simulations start from a spin-up simulation where equilibrium was reached; i.e., the CTRL simulation is a continuation of this spin-up run. We use ECHAM6 in T63L47 resolution (T63: spectral truncation at wave number 63, roughly corresponding to 1.9° horizontal resolution; L47: 47 vertical levels). In this setup ECHAM6 extends from the surface to 0.01 hPa. The high vertical resolution in our simulation setup allows for a detailed representation of the dynamical processes driving the BDC [Bunzel and Schmidt, 2013; Charlton-Perez *et al.*, 2013]. Sea surface temperatures and sea ice distribution were taken from the MPI-ESM “1pctCO2” simulation that has been conducted within the framework of the Coupled Model Intercomparison Project phase 5 (CMIP5) project [Taylor *et al.*, 2012; Giorgetta *et al.*, 2013]; i.e., they are transiently changing in 1PCT and are kept constant at the starting year distribution of “1pctCO2” in CTRL. CO_2 concentrations were prescribed with yearly 1% increase in 1PCT, starting at the preindustrial level of 285 ppm, that is kept constant in CTRL. Atmospheric N_2O concentrations are simulated interactively. Ozone, aerosols, and all other greenhouse gases except for CO_2 and N_2O were kept constant at their preindustrial concentrations in both simulations. As ECHAM6 does not contain atmospheric chemistry, and as we focus on the effect of the changing circulation, stratospheric decay rates of N_2O are prescribed as a function of longitude, latitude, and atmospheric level. Stratospheric decay rates are taken from a MOZART-3 (Model of Ozone and Related Chemical Tracers) simulation for the year 2008 performed within the European project Monitoring of Atmospheric Composition and Climate [Kinnison *et al.*, 2007; Stein *et al.*, 2012]. For the MOZART-3 simulation, all gas-phase reaction rates as well as the absorption cross sections and quantum yields for the photolytic reactions had been updated to the 2011 estimates by the NASA Jet Propulsion Laboratory [Sander *et al.*, 2011].

Natural emissions of N_2O are sensitive to climatic conditions and are thus affected by climate change. In order to avoid these side effects, we prescribe N_2O emissions as constant at pre-industrial rates. Thereby, we avoid artificially pinned surface N_2O concentrations and thus see the full signal in atmospheric concentration changes induced by the changes in the stratospheric sink throughout the full atmospheric column. Prescribing emissions and not concentrations in future climate change scenarios is a new feature in our study as compared to, e.g., the study by Chipperfield *et al.* [2014] focusing on the historical period. We prescribe surface N_2O fluxes in both the CTRL and the 1PCT simulation with $10.4 \text{ Tg N}_2\text{O-N yr}^{-1}$ from a preindustrial MPI-ESM simulation. Atmospheric N_2O concentrations in the CTRL simulation (276 ppbv)—equivalent to the starting conditions for 1PCT—are at preindustrial values [Syakila and Kroeze, 2011].

3. Results

To diagnose the strength of the BDC in our simulations, we compute the residual mean vertical velocity at the 70 hPa level, characterizing vertical mass transport by the BDC. The residual mean vertical velocity w^* is calculated following the transformed Eulerian mean framework, which approximates the Lagrangian-mean mass transport [Andrews *et al.*, 1987; Butchart, 2014]. Results for the CTRL simulation and the final 10 years of the 1PCT simulation are shown in Figure 1a. In 1PCT, the simulated global mean surface temperatures increase by approximately 3 K (Figure S1 in the supporting information). The increased upwelling in the tropics and the increased downwelling in the extratropics demonstrate an accelerated stratosphere-troposphere exchange and agrees with predictions by other models [e.g., Butchart *et al.*, 2006; Hardiman *et al.*, 2014]. Evolution of the BDC can be illustrated by calculating the total tropical upward mass flux, which is a global indicator for the strength of the BDC. The tropical mass flux across the 70 hPa pressure level is calculated by the area weighted integral of the residual mean vertical velocity times the air density. By using log-pressure coordinate scaling [Andrews *et al.*, 1987], the density at 70 hPa is given by $p S^{-1} g^{-1}$ where S is the scale height (7000 m), g the gravity (9.81 m s^{-2}), and p the pressure (70 hPa). The mass flux was calculated for tropical grid cells with w^* directed upwards ($w^* > 0$). In the 1PCT simulation the tropical upward mass flux increases almost linearly (Figure 1b)—in line with the global mean temperature change (Figure S1)—by about 35% during the 100 simulated

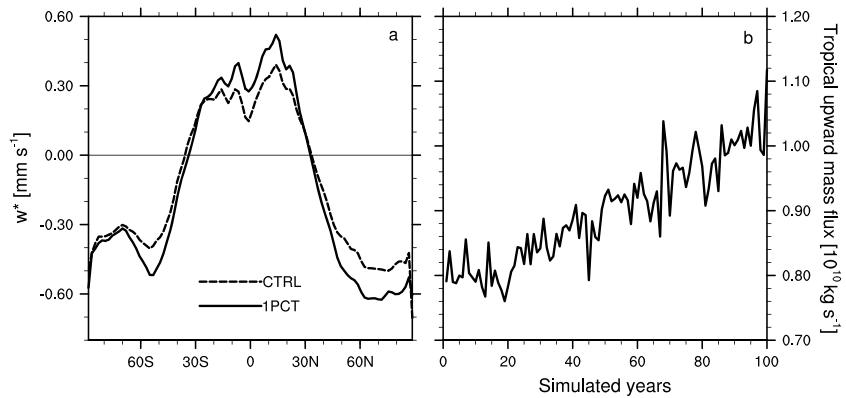


Figure 1. (a) Annual and zonal mean residual vertical velocity w^* at 70 hPa averaged for 10 years for the CTRL simulation and the final 10 years of the 1PCT simulation and (b) annual upward mass flux in the tropics for the 1PCT simulation.

years. The accelerated atmospheric circulation affects N_2O distribution and burden. In the 1PCT simulation, tropospheric N_2O concentration decreases while stratospheric concentration increases (Figure 2a), such that, by the end of the 1PCT simulation, the distribution of N_2O in the atmosphere is distinctly different from the CTRL simulation (Figure 2a). The modified distribution of N_2O in the atmosphere leads to an increase in the amount of N_2O being destroyed in the stratosphere. This is due to the fact that photolytic rates are strongest in the tropical region. Here more N_2O is transported from the troposphere into the stratosphere and thus available for stratospheric decay (Figure 2b).

3.1. Decline in N_2O Burden and Implications for Total Radiative Forcing

Given the constant emissions in our setup the increase in the N_2O sink (Figures 3a and 3e) leads to a reduction in its burden (Figures 3b and 3f) of 5% within the 100 simulated years in 1PCT. The overall decline of N_2O affects its total radiative forcing. Calculated as a product of the change in N_2O burden and the radiative efficiency of N_2O (see below), a 5% reduction in the burden leads to a reduction in the total radiative forcing of N_2O of 0.04 W m^{-2} . This value corresponds to 24% of the currently assumed radiative forcing of anthropogenic N_2O (0.17 W m^{-2}) [Myhre et al., 2013a]. In a simulation setup with prescribed constant concentrations instead of surface emissions, this effect would have been masked as prescribing constant concentrations prevent changes in burden and imply increasing N_2O emissions sustaining those concentrations. The difference between prescribing surface emissions versus concentrations has already been examined for the historical period by Chipperfield et al. [2014] who, in accordance with our study, found that it affects

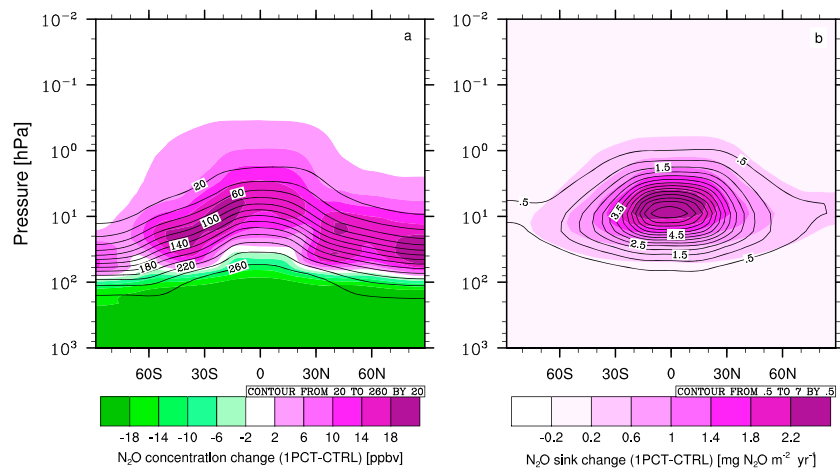


Figure 2. (a) Zonal mean N_2O concentrations (ppbv) and (b) N_2O sink ($\text{mg N}_2\text{O m}^{-2} \text{ yr}^{-1}$) as simulated in the CTRL simulation (contours) and the differences between the averaged final 10 years of the 1PCT simulation and the CTRL simulation (colors).

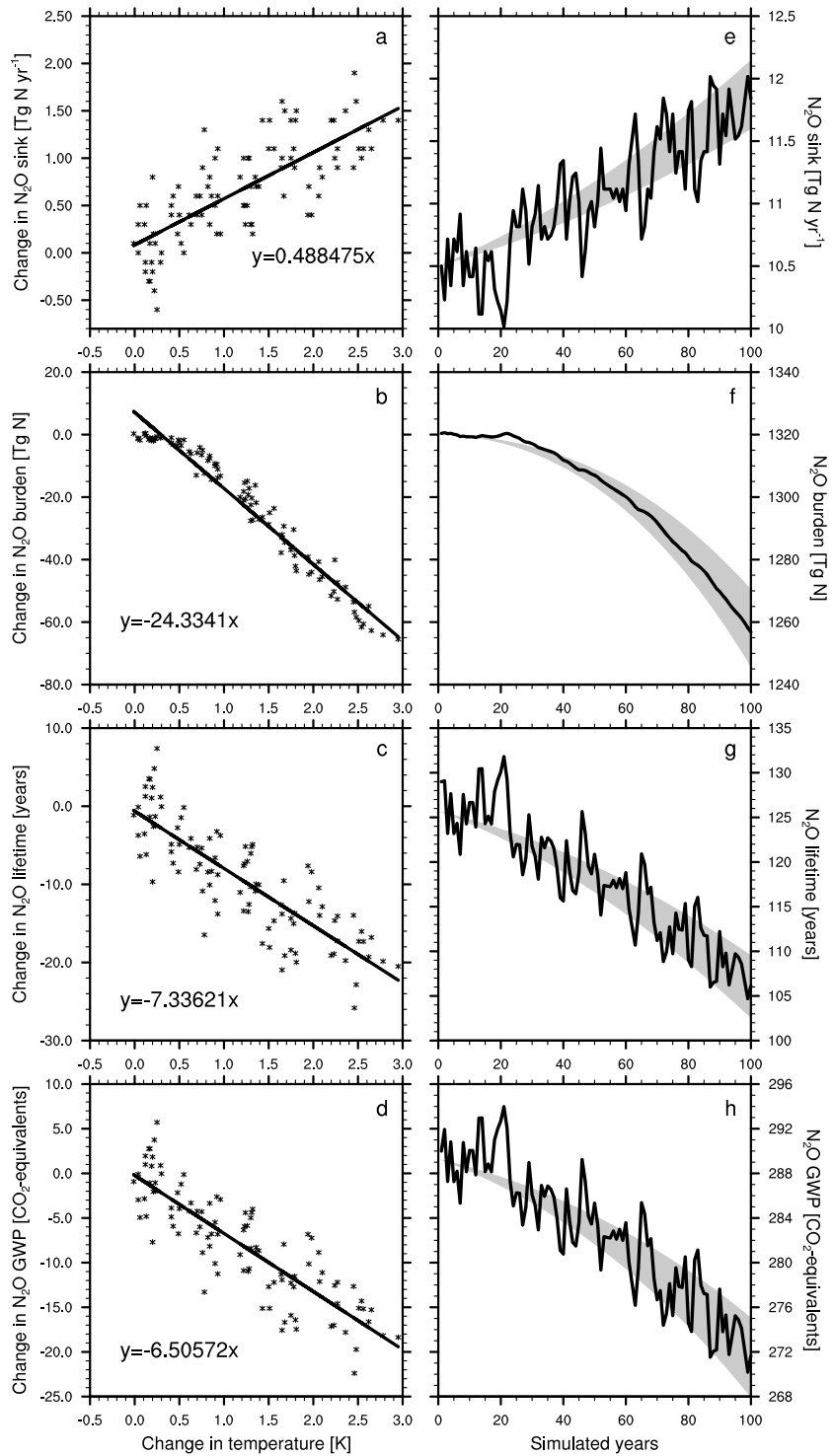


Figure 3. (a–d) Changes in atmospheric N₂O characteristics (1PCT-CTRL) versus changes in global annual mean surface temperature and the fitted regressions. (e–h) Evolution of atmospheric N₂O characteristics with time in the 1PCT simulation (solid line). Grey areas depict model uncertainty range. Evolution of variables for lower and upper bound for uncertainty range is calculated by functions described in equations (S1) to (S3) in the supporting information.

atmospheric burden, but not lifetime. With our study we can further emphasize the importance of prescribing surface flux boundary conditions particularly under a global warming scenario with enhanced BDC.

3.2. Reduction in N₂O GWP With Declining Lifetime

The enhanced sink of N₂O induced by the accelerated BDC reduces its residence time in the atmosphere and thus its efficacy as a greenhouse gas. The atmospheric lifetime (τ) of a substance is obtained from its atmospheric burden (B) and its sink strength (S) by

$$\tau(t) = B(t)/S(t). \quad (1)$$

Since we want to compute how the N₂O lifetime changes under climate change, we already introduce a time dependence in this formula, well knowing that this is valid only as long as the change in burden and sink is sufficiently slow. With enhanced circulation, more N₂O is available in the stratosphere relative to the total atmospheric burden; i.e., the sink term is increased relative to the burden, leading to a reduction in τ . In the 1PCT simulation the so calculated N₂O lifetime decreases to 105 years after 100 simulation years (Figure 3g), corresponding to a 14% reduction relative to a value of 127 ± 2.5 years in CTRL. This reduction in lifetime due to the enhanced BDC is comparable to the one *Fleming et al.* [2011] found for the Special Report on Emissions Scenarios A1B scenario.

We quantify the effect of a reduced lifetime on the climatic relevance of N₂O by calculating its global warming potential (GWP). The GWP is a measure to normalize the climate efficiencies of greenhouse gases (GHGs) relative to that of CO₂. This allows for a comparison of different GHG emissions according to their relevance for global warming [*Bows-Larkin et al.*, 2014]. It is also applied in assessing the efficiency of mitigation strategies and has been used by *Crutzen et al.* [2007] to reveal potential offsets of the CO₂ sequestration of biofuel plantations by additional emissions of N₂O. The GWP of a GHG is defined as the ratio of its absolute global warming potential (AGWP) to the AGWP of CO₂. The AGWP of a GHG is the radiative forcing resulting from 1 kg additionally emitted GHG integrated over a time horizon H . In the calculation of the GWP as defined in the Intergovernmental Panel on Climate Change (IPCC) report [*Myhre et al.*, 2013a; 2013b], the lifetime of N₂O is used to calculate the remaining amount [N₂O(t)] of the emitted kilogram at time t with an exponential function: [N₂O(t)] = $e^{-t/\tau}$. Describing the atmospheric abundance with an e -fold approach demands a lifetime that is constant in space and time [*Ehhalt et al.*, 2001]. As τ is reduced under global warming, we consider $\tau(t)$ of the year $t=y$ when emissions occur

$$\text{GWP}_{\text{N}_2\text{O}}(y) = \frac{\int_y^{y+H} a_{\text{N}_2\text{O}} [\text{N}_2\text{O}(t)] dt}{\text{AGWP}_{\text{CO}_2}(H)} = \frac{a_{\text{N}_2\text{O}} \tau(y) \left(1 - e^{-\frac{H}{\tau(y)}}\right)}{\text{AGWP}_{\text{CO}_2}(H)} \quad (2)$$

where $a_{\text{N}_2\text{O}}$ is the radiative efficiency of N₂O ($0.003 \text{ W m}^{-2} \text{ ppbv}^{-1}$ or $3.85\text{e-}13 \text{ W m}^{-2} \text{ kg}^{-1}$) [*Myhre et al.*, 2013b]. Due to the long lifetime of N₂O, we choose a time horizon of $H=100$ years for integrating the radiative forcing. For this time horizon we calculate a N₂O GWP of 290 ± 2 CO₂-equivalents for the CTRL simulation. This value is similar to the currently assumed present-day N₂O GWP of 298 CO₂-equivalents [*Myhre et al.*, 2013a].

In equation (2), the remaining amount of the emitted kilogram at time t is calculated with an exponential function. Hence, when adapting the IPCC approach to calculate the AGWP, the lifetime of N₂O needs to be considered constant in equation (2). By considering $\tau(t)$ computed from equation (1) for a particular year $t=y$ of our 1PCT simulation, the resulting GWP of N₂O refers to the kilogram of N₂O emitted in that year assuming that the lifetime will stay constant for the subsequent years during the time horizon H . Choosing a time horizon of $H=100$ years, we thus derive a time series of N₂O GWP (Figure 3h). In the 1PCT simulation the so calculated GWP decreases to 272 CO₂-equivalents for N₂O emitted in year 100 (see Figure 3h). Since we know that τ decreases in the 1PCT simulation, and that it in fact also decreases during the time horizon that is chosen for integrating the radiative forcing, the reduction of the N₂O GWP due to a reduced lifetime actually must be larger. We consider this by applying an alternative approach that is described in the following.

The GWP plotted in Figure 3h starts from a value similar to the value obtained from the CTRL simulation reflecting the fact that lifetime has been kept constant during the time horizon, which mimics the behavior of the control simulation, where anyway τ is constant. Considering all 100 years of the 1PCT simulation data this value for $t=0$ can be improved by explicitly accounting for the degradation of the emitted kilogram N₂O during the time horizon. We describe this degradation by an additional

alternative calculation. Thereby, we determine the remaining amount of the emitted mass not with an exponential function, but by calculating the yearly sink of N_2O by equation (1) and subtracting it from the remaining amount of the emitted kilogram in the previous year: $N_2O(t + dt) = N_2O(t) - dN_2O(t)/dt$ with dN_2O/dt being the sink of N_2O : $dN_2O/dt = N_2O(t)/\tau(t)$. When calculating $[N_2O(t)]$ and the GWP with this alternative approach, the GWP of N_2O emitted in the first year of the 1PCT simulation is 286 CO_2 -equivalents. Hence, when calculating the N_2O GWP, a change in the N_2O lifetime is important and can be taken into account in different ways changing the strength of the signal.

To provide an idea on how an enhanced BDC can affect the lifetime and the GWP of N_2O in a more realistic climate projection, we apply our findings to the temperature evolution of the Representative Concentration Pathway (RCP) 8.5 scenario. For RCP8.5, global mean temperatures increase by 3.5° from 2006 to 2100 as simulated by MPI-ESM, which is a similar temperature increase as in our 1PCT simulation. In a multimodel comparison study including the MPI-ESM, *Hardiman et al.* [2014] found an increase of 3.5% per decade in tropical upwelling for the RCP8.5 scenario, which is also similar to the increase we find. Applying the temperature regressions shown in Figure 3 to this temperature rise, the lifetime of N_2O is reduced from a present-day lifetime of 131 years to 98.8 years in 2100. Using these lifetimes to calculate the GWP according to equation (1), the N_2O GWP is reduced from 293 CO_2 -equivalents at present day by 9% to 267 CO_2 -equivalents in the year 2100. The MPI-ESM RCP8.5 simulation conducted for the CMIP5 project covers the time period 2005–2200. Hence, we can apply the alternative approach (considering a changing τ for the integration) to calculate the GWP for N_2O emitted in year 2100. The lifetime of N_2O , determined by applying the linear regression with temperature rise, further decreases for the RCP8.5 scenario to 68.3 years until the year 2200. The so calculated GWP for N_2O emitted in the year 2006 is 284 CO_2 -equivalents, and for N_2O emitted in the year 2100 it is reduced by 12% to 251 CO_2 -equivalents.

In our study we focus on the implications of the acceleration of the BDC on N_2O lifetime and the resulting effects for climate change by diagnosing a decrease in its GWP. In addition to a change in the circulation, the lifetime of N_2O can also be affected by other factors. N_2O is mainly destroyed by photolysis and to a minor fraction by reaction with excited oxygen, thereby contributing to ozone destruction. The strength of photolysis depends on the amount of ozone, i.e., increasing ozone concentrations due to ozone recovery as a result of the reduction in CFCs means that less radiation can penetrate and that photolytic rates decrease. Other modeling studies have for instance found that this effect can compensate for [*Chipperfield et al.*, 2014] or be marginal [*Fleming et al.*, 2011; *Douglass et al.*, 2008] compared to the effect of an enhanced BDC on the lifetimes of ODS.

As N_2O is an important ODS, it feeds back on its own lifetime by reducing ozone and thus enhancing the photolytic rates. *Hsu and Prather* [2010] for instance found a thus induced decrease in the N_2O lifetime of 10 years, and *Prather and Hsu* [2010] found a decrease in N_2O radiative forcing by 8% due to this effect. The IPCC reported that for every 10% increase in N_2O , its global mean atmospheric lifetime will be reduced by 0.5% [*Ehhalt et al.*, 2001] due to feedback via ozone destruction. The destruction of ozone due to N_2O on the other hand has been shown to be buffered by the thermal effect of CO_2 by 20% until 2100 for the A1 scenario by *Portman et al.* [2012]. In addition, there is a link between N_2O and ozone via CH_4 . *Prather and Hsu* [2010] examine the effect of a N_2O pulse emissions on CH_4 via ozone destruction and related changes in the hydroxyl radical. They state that the N_2O radiative forcing is reduced by 4.5% due to an implied decrease in CH_4 . Due to its linkage to halocarbons, methane buffered the destruction of ozone by 20% [*Portman et al.*, 2012]. *Hsu and Prather* [2010] found that this effect leads to a 1.2% increase in the CH_4 GWP due to a reduced decay of N_2O with reduced ozone concentration.

In the calculation of the GWP the AGWP of CO_2 is used as a reference. As the background concentration of CO_2 raises, and due to climate-carbon feedback, the AGWP of CO_2 will change under climate change. *Reisinger et al.* [2011] project an increase in the N_2O GWP due to changes in the AGWP of CO_2 of 20% for the RCP8.5 scenario. As shown in *Myhre et al.* [2013a], the N_2O GWP decreases by ~ 30 CO_2 -equivalents when climate-carbon feedback are not considered.

Hence, the values for lifetime and GWP we derive are not thought to be a realistic prediction. They illustrate the importance of a change in atmospheric dynamics for the climate efficacy of N_2O and can, in follow-up studies, be helpful to assess the relative contribution of the BDC for a simulation considering more factors.

3.3. Linear Regressions With Temperature Change

In the present study we isolate the impact of an accelerated BDC on variables describing the atmospheric fate of N₂O. The evolution of N₂O sink, burden, lifetime, and GWP can be approximated by linear regressions against temperature increase as demonstrated in Figures 3a–3d. We find an increase in yearly N₂O sink of 0.5 Tg N K⁻¹, leading to a decrease in N₂O burden of 24 Tg N K⁻¹ and in N₂O lifetime of 7.3 yr K⁻¹. The GWP of N₂O calculated with equation (2) is reduced by 6.5 CO₂-equivalents K⁻¹. These regressions also replicate the trend in atmospheric N₂O characteristics for a simulation with slowed global warming (supporting information). Hence, by describing the evolution of the atmospheric N₂O characteristics as functions of temperature increase, our findings can be applied to different speeds of temperature rise and are not restricted to one particular scenario. Such a restriction is usually the case in other studies providing results as changes per time period, e.g., per decade [e.g., *Hardiman et al.*, 2014]. Our assessment is based on a CO₂-induced climate change. Given that CO₂ is the dominant forcing for anthropogenic climate change and that the increase in tropospheric temperatures has been found to be the main driver of the acceleration in the BDC [*Sigmond et al.*, 2004; *Chen et al.*, 2010; *Oberländer et al.*, 2013], we are positive that our findings can be extended to realistic climate change scenarios, even though the mechanism for the acceleration of the BDC is more complex.

The acceleration of the BDC is simulated differently by different models [*Butchart et al.*, 2006]. To mirror the intermodel uncertainty in the BDC prediction, we describe N₂O burden, lifetime, and GWP as functions of the N₂O sink and its sensitivity k to temperature change (for details see supporting information). We choose this approach because the increase in N₂O sink is the key factor inducing the simulated alterations in N₂O burden, lifetime, and GWP. Models simulating different acceleration of the BDC would also simulate a different k ; i.e., by varying k we can estimate a model range (grey area in Figures 3e–3h). In a multimodel comparison study diagnosing simulated acceleration of BDC by w^* *Hardiman et al.* [2014] found an intermodel standard error of approximately 20% of the multimodel mean. This spread includes the difference in BDC due to different warming rates as well as due to different circulation responses given the same temperature increase. It can thus be seen as an upper bound for the spread in the BDC. As MPI-ESM is found approximately in the middle of the model ensemble range in that analysis, varying k by 20% is assumed to be appropriate to represent the uncertainty due to different model parameterizations. The uncertainties calculated by this approach are small compared to the overall effect of the enhanced BDC under global warming (Figures 3e–3h).

4. Conclusion

In our analysis, we examine climate-N₂O interactions via a change in atmospheric dynamics and find a decrease in the N₂O lifetime, burden, and GWP, induced by an enhanced BDC.

A reduction in N₂O GWP implies that the climatic impact of N₂O emissions is smaller under global warming and that the relative importance of N₂O emissions compared to emissions of other GHGs might change, depending on how other GHGs change in the future. As the radiative efficiency of one molecule N₂O is 26 times higher than that of CO₂, and as its lifetime is long even under an accelerated BDC, N₂O will remain an important target for mitigation options. However, with declining lifetime of N₂O, strategies to reduce N₂O emissions might not be as efficient in mitigating climate change as originally assumed.

The effect of an accelerated BDC on the atmospheric fate of N₂O, namely, a reduction in its burden, is important to assess the total radiative forcing of N₂O. When N₂O emissions are converted to concentrations without considering this effect, the relevance of those emissions for climate change will be overestimated. Whenever N₂O emissions are translated to concentrations or the other way round, e.g., for generating concentration scenarios, not considering a changing lifetime will lead to inaccuracies. But also beyond a perspective strictly related to climate change, this aspect is relevant. An overestimation of the N₂O burden would for instance also lead to wrong conclusions regarding ozone destruction.

The extent to which the N₂O lifetime will change under climate change depends not only on the change in atmospheric dynamics but also on various complex chemical interactions and their evolution. For an exact prediction on the development of the N₂O lifetime and burden and its effect for climate change, chemistry-climate simulations with surface flux boundary conditions would be needed. However, for such simulations several partly uncertain assumptions would be necessary restricting the results to those assumptions. The effect of

the enhanced BDC on the lifetime of N₂O will be stronger with higher temperatures and is thus dependent on the chosen climate scenario. Here our findings can be used in further investigations to assess the relevance of the BDC on the N₂O lifetime compared to other effects under different global warming scenarios.

Correlations between future temperature increase and N₂O have so far only been considered focusing on N₂O emissions and potential feedback to climate change. In our study we open a new perspective on the climate-N₂O interactions as we show that temperature change can affect the relevance of N₂O for climate change also via an atmospheric signal.

Acknowledgments

We thank Felix Bunzel for providing the scripts for the TEM diagnostic. This work was funded by the European Union, Seventh Framework Programme (FP7/2007–2013) in the COMBINE project and by the German Science Foundation (DFG) in the Priority Programme (SPP) 1689. The simulations were performed on the computer of the German Climate Computing Center (DKRZ). Data and scripts used for and data produced during the analysis are archived by the Max Planck Institute for Meteorology and can be obtained by contacting publications@mpimet.mpg.de.

References

- Andrews, D. G., J. R. Holton, and C. B. Leovy (1987), *Middle Atmosphere Dynamics*, Academic Press, San Diego, Calif.
- Bows-Larkin, A., C. McLachlan, S. Mander, R. Wood, M. Röder, E. Dawkins, C. Gough, L. O. Keefe, and M. Sharmina (2014), Importance of non-CO₂ emissions in carbon management, *Carbon Manag.*, 5(2), 37–41, doi:10.1080/17583004.2014.913859.
- Bunzel, F., and H. Schmidt (2013), The Brewer–Dobson circulation in a changing climate: Impact of the model configuration, *J. Atmos. Sci.*, 70(5), 1437–1455, doi:10.1175/JAS-D-12-0215.1.
- Butchart, N. (2014), The Brewer–Dobson circulation, *Rev. Geophys.*, 52, 157–184, doi:10.1002/2013RG000448.
- Butchart, N., and A. Scaife (2001), Removal of chlorofluorocarbons by increased mass exchange between the stratosphere and troposphere in a changing climate, *Nature*, 410, 799–802.
- Butchart, N., et al. (2006), Simulations of anthropogenic change in the strength of the Brewer–Dobson circulation, *Clim. Dyn.*, 27(7–8), 727–741, doi:10.1007/s00382-006-0162-4.
- Charlton-Perez, A. J., et al. (2013), On the lack of stratospheric dynamical variability in low-top versions of the CMIP5 models, *J. Geophys. Res. Atmos.*, 118, 2494–2505, doi:10.1002/jgrd.50125.
- Chen, G., A. Plumb, and J. Lu (2010), Sensitivity of zonal mean atmospheric circulation to SST warming in an aqua-planet model, *Geophys. Res. Lett.*, 37, L12701, doi:10.1029/2010GL043473.
- Chipperfield, M. P., et al. (2014), Multimodel estimates of atmospheric lifetimes of long-lived ozone-depleting substances: Present and future, *J. Geophys. Res. Atmos.*, 119, 2555–2573, doi:10.1002/2013JD021097.
- Crutzen, P. J., A. R. Mosier, K. A. Smith, and W. Winiwarter (2007), N₂O release from agro-biofuel production negates global warming reduction by replacing fossil fuels, *Atmos. Chem. Phys. Discuss.*, 7(4), 11,191–11,205, doi:10.5194/acpd-7-11191-2007.
- Dougllass, A. R., R. S. Stolarski, M. R. Schoeberl, C. H. Jackman, M. L. Gupta, P. A. Newman, J. E. Nielsen, and E. L. Fleming (2008), Relationship of loss, mean age of air and the distribution of CFCs to stratospheric circulation and implications for atmospheric lifetimes, *J. Geophys. Res.*, 113, D14309, doi:10.1029/2007JD009575.
- Ehalt, D., et al. (2001), Atmospheric chemistry and greenhouse gases, in *Climate Change 2001: The Physical Science Basis, Contribution to Working Group I of the Fifth Assessment Report of the Intergovernmental Panel on Climate Change*, edited by J. T. Houghton et al., Cambridge Univ. Press, Cambridge, U. K., and New York.
- Fleming, E. L., C. H. Jackman, R. S. Stolarski, and A. R. Douglass (2011), A model study of the impact of source gas changes on the stratosphere for 1850–2100, *Atmos. Chem. Phys.*, 11(16), 8515–8541, doi:10.5194/acp-11-8515-2011.
- Giorgetta, M. A., et al. (2013), Climate and carbon cycle changes from 1850 to 2100 in MPI-ESM simulations for the Coupled Model Intercomparison Project phase 5, *J. Adv. Model. Earth Syst.*, 5, 572–597, doi:10.1002/jame.20038.
- Hardiman, S. C., N. Butchart, and N. Calvo (2014), The morphology of the Brewer–Dobson circulation and its response to climate change in CMIP5 simulations, *Q. J. R. Meteorol. Soc.*, doi:10.1002/QJ.2258.
- Hsu, J., and M. J. Prather (2010), Global long-lived chemical modes excited in a 3-D chemistry transport model: Stratospheric N₂O, NO_y, O₃ and CH₄ chemistry, *Geophys. Res. Lett.*, 37, L07805, doi:10.1029/2009GL042243.
- Kinnison, D. E., et al. (2007), Sensitivity of chemical tracers to meteorological parameters in the MOZART-3 chemical transport model, *J. Geophys. Res.*, 112, D20302, doi:10.1029/2006JD007879.
- Myhre, G., et al. (2013a), Anthropogenic and natural radiative forcing, in *Climate Change 2013: The Physical Science Basis. Contribution to Working Group I to the Fifth Assessment Report of the Intergovernmental Panel on Climate Change*, edited by T. F. Stocker et al., Cambridge Univ. Press, Cambridge, U. K., and New York.
- Myhre, G., et al. (2013b), Supplementary Material. Anthropogenic and natural radiative forcing, in *Climate Change 2013: The Physical Science Basis. Contribution to Working Group I to the Fifth Assessment Report of the Intergovernmental Panel on Climate Change*, edited by T. F. Stocker et al., Cambridge Univ. Press, Cambridge, U. K., and New York.
- Neu, J. L., T. Flury, G. L. Manney, M. L. Santee, N. J. Livesey, and J. Worden (2014), Tropospheric ozone variations governed by changes in stratospheric circulation, *Nat. Geosci.*, 7(5), 340–344, doi:10.1038/ngeo2138.
- Oberländer, S., U. Langematz, and S. Meul (2013), Unraveling impact factors for future changes in the Brewer–Dobson circulation, *J. Geophys. Res. Atmos.*, 118, 1–17, doi:10.1002/jgrd.50775.
- Portman, R. W., J. S. Daniel, and A. R. Ravishankara (2012), Stratospheric ozone depletion due to nitrous oxide: Influences of other gases, *Philos. Trans. R. Soc. Ser. B*, 367, 1256–1264, doi:10.1098/rstb.2011.0377.
- Prather, M. J., and J. Hsu (2010), Coupling of nitrous oxide and methane by global atmospheric chemistry, *Science*, 330, 952–954, doi:10.1126/science.1196285.
- Ravishankara, A. R., J. S. Daniel, and R. W. Portman (2009), Nitrous oxide (N₂O): The dominant ozone-depleting substance emitted in the 21st century, *Science*, 326, 123–125.
- Reisinger, A., M. Meinshausen, and M. Manning (2011), Future changes in global warming potentials under representative concentration pathways, *Environ. Res. Lett.*, 6, 024020, doi:10.1088/1748-9326/6/2/024020.
- Sander, S. P., et al. (2011), Chemical kinetics and photochemical data for use in atmospheric studies, evaluation number 17.
- Sigmond, M., P. C. Siegmund, E. Manzini, and H. Kelder (2004), A simulation of the separate climate effects of middle-atmospheric and tropospheric CO₂ doubling, *J. Clim.*, 17, 2352–2367.
- Stein, O., J. Flemming, A. Inness, J. W. Kaiser, and M. G. Schultz (2012), Global reactive gases forecasts and reanalysis in the MACC project, *J. Integr. Environ. Sci.*, 9, 57–70, doi:10.1080/1943815X.2012.696545.

- Stevens, B., et al. (2013), The atmospheric component of the MPI-ESM: ECHAM6, *J. Adv. Model. Earth Syst.*, 5, 146–172, doi:10.1002/jame.20015.
- Syakila, A., and C. Kroeze (2011), The global nitrous oxide budget revisited, *Greenh. Gas Meas. Manag.*, 1(1), 17–26, doi:10.3763/ghgmm.2010.0007.
- Taylor, K. E., R. J. Stouffer, and G. A. Meehl (2012), An overview of CMIP5 and the experiment design, *Bull. Am. Meteorol. Soc.*, 93(4), 485–498, doi:10.1175/BAMS-D-11-00094.1.